



Computational Fluid Dynamics analysis applied to engineering and design of poultry farms

Eva H. Guerra-Galdo¹, Fernando Estellés Barber¹, Salvador Calvet Sanz¹,
P. Amparo López-Jiménez²

¹ Institute of Animal Science and Technology, Universitat Politècnica de València. Camino de Vera s/n. 46022 Valencia, Spain.

² Hydraulic and Environmental Engineering Department. Universitat Politècnica de València. Camino de Vera s/n. 46022 Valencia, Spain.

Abstract

The shape of a poultry building and the distribution of its elements (roof, windows distribution, and window opening) influence the velocity and temperature distribution inside the building and therefore the thermal comfort of the broilers. Considering these components, Computational Fluid Dynamics (CFD) was used to analyze the environmental conditions of 3 poultry buildings: tunnel (T), semi-tunnel (ST) and improved semi-tunnel (IST). These three buildings had the same dimensions but differed in the relative position of fans and windows. This study modelled the effect of different configurations of roof (flat or gable roof) and window design (with or without flap plate) on the distribution of temperature, air velocity and Index of Temperature and Velocity (ITV) at animal level (0.20 m above the ground). Simulations were conducted for summer and winter conditions. In summer conditions, configuration IST with gable roof without flap plate had lowest air velocity 0.72 ± 0.27 m/s and average temperature ($22.9\pm 0.9^\circ\text{C}$) whereas tunnel configuration with gable roof and flap plate had lowest ITV ($22.94\pm 1.30^\circ\text{C}$ on average). In winter conditions, IST configuration with flat roof had lowest average air velocity (0.24 m/s), whereas the highest temperature corresponded to semi-tunnel with gable roof without flap plate of the slot opening ($19.35\pm 2.67^\circ\text{C}$). Finally, the lowest ITV corresponded to tunnel without flap plate and gable roof configuration ($19.14\pm 3.57^\circ\text{C}$). According to the CFD simulations, in three configurations the variables analyzed were within the comfort ranges reported for animals inside buildings.

Copyright © 2016 International Energy and Environment Foundation - All rights reserved.

Keywords: Broiler building; Computational Fluid Dynamics; Temperature; Velocity; Comfort.

1. Introduction

The growing demand for animal protein has increased in accordance with population growth. For this reason, genetic selection produces permanent changes in the production parameters of broilers, including feed efficiency and growth, but also the tolerance for changing environmental conditions. In this sense, in order to take advantage of the productive potential of broilers, we must control the environment throughout the year, and provide adequate environmental parameters of temperature $21\text{-}23^\circ\text{C}$ [1], air velocity $1.5\text{-}2.0$ m/s [2, 3] and humidity $60\text{-}65\%$ [4] at the end of the growing period. To manage these factors, the livestock farm should be appropriately designed and operated for different stages of development and seasons.

The farm engineering design affects its performance in terms of production and profitability, by providing an optimum environmental control to enhance productivity. To achieve such optimization, the use of technology is necessary to adapt to summer conditions. This technology includes the use of different ventilation systems as well as other engineering strategies such as internal water misting [5], different sizes and positions of air inlets; and lowering the roof all along the poultry building to increase air velocity [6, 7]. In winter conditions, however, the need is to maintain an appropriate temperature and at the same time to exhaust the noxious gases. To obtain a higher uniformity of environmental conditions at the broiler zone, design proposals include installing multiple openings [8], using both sidewall and ceiling air inlets [9]; or using chimney inlets with diffuser and a side-up outlet at the eave [10].

To predict the thermal response of animals to different installation designs and operations, simulations of realistic conditions must be done by means of the use of computational fluid dynamics (CFD) based on numerical solutions. By doing so, air properties, airflow conditions, heat and mass sources can be simultaneously represented. The final objective is to predict the temperature distribution in the broilers production environment, as well as the gas concentration and other physical properties of particular livestock buildings [5, 9, 11, 12].

CFD simulations can be used by designers as a virtual laboratory to take decisions. Therefore, the hypothesis of this study is based on the variation of certain design elements of the farm: number and location of fans operating [11]; inlet and outlet surface of the openings [9]; wind velocity and direction considerations, the temperature differences between the indoor and outdoor environment [10]; shape of the roof of the building; relative position and size the slots opening height, flap plate angle at the air inlet windows [7, 8, 12, 13]. The influence of equipment installation and the presence of birds [14, 15] could be considered as well.

Therefore, the main objective of this study is to simulate by means of CFD analysis, different configurations of poultry houses in summer and winter conditions by analyzing three different geometry proposals. Parameters under analysis will be changed: (roof slope, window distribution and slot openings) to evaluate changes in temperature and ventilation patterns inside the farm and demonstrating the capability of the simulation software to be used as a tool for comparison between different designs.

2. Materials and methods

2.1 Farm description: Geometry and configuration of windows

The geometry of three broiler buildings has been considered: Classical tunnel type (T), semi-tunnel (ST) and improved semi-tunnel (IST), all them measuring 15m wide, 120m long, 3m high walls and differing in roof shape (flat roof or gable roof of 5m ridge height, Figure 1) as description in Table 1.

Different fans were considered to be in operation for summer and winter conditions. The air was exhausted from the building during the summer period by means of eight fans of 1.40m diameter (airflow 38,072, m³/h) and two fans of 1.10m diameter (13,406 m³/h). These exhaust fans created a negative pressure forcing air to enter through inlet windows of 0.9m x 0.4m. At the same time, different distributions of windows with or without flap plates were considered. In the winter period a different distributions of fans was considered, using only two fans of 1.10m diameter (13,406 m³/h), with different distributions of windows adopting fixed flap plate angles of the slots.

2.1.1 Description broiler building in summer

An outside temperature of 21.5°C was considered for summer conditions and then, the three configurations (T, ST and IST) were compared. For each design, changes were simulated in the distribution of windows and fans, roof shape (flat and gable) and slot opening with or without flap plate, as described in Table 2. In the three configurations we used flat roof (f), but only slot opening without flap plate was considered (S/O Tf_s, S/O STf_s and S/O ISTf_s), as well as and flaps in the window openings (F/P) with a 0° angle (F/P Tf_s, F/P STf_s and F/P ISTf_s). The same configurations were used for gable roof (g), without flaps (S/O Tg_s, S/O STg_s, S/O ISTg_s) and with flaps (F/P Tg_s, F/P STg_s, F/P ISTg_s).

2.1.2 Description broiler building in winter

During the winter period (outdoor temperature 5°C) we considered a lower ventilation rate using two exhaust fans. We considered the three configurations mentioned before (T, ST and IST) with flat roof (f), both considering slot open windows (S/OTf_w, S/OSTf_w, S/O ISTf_w), and considering flap plates (82° angle) (F/P Tf_w, F/P STf_w, F/P ISTf_w). For gable roof, similar configurations were tested (S/OTgw,

S/OSTgw, S/OISTgw). As shown Table 2, geometries were simulated for any configuration either in summer and winter conditions.

To model incidence flap plate angle we used the IST_{gw} configuration and windows opened gradually at six different flap plates angles in the slots openings (0°, 55.2°, 73.9°, 82°, 85.4°, 89.12°) (Figure 2).

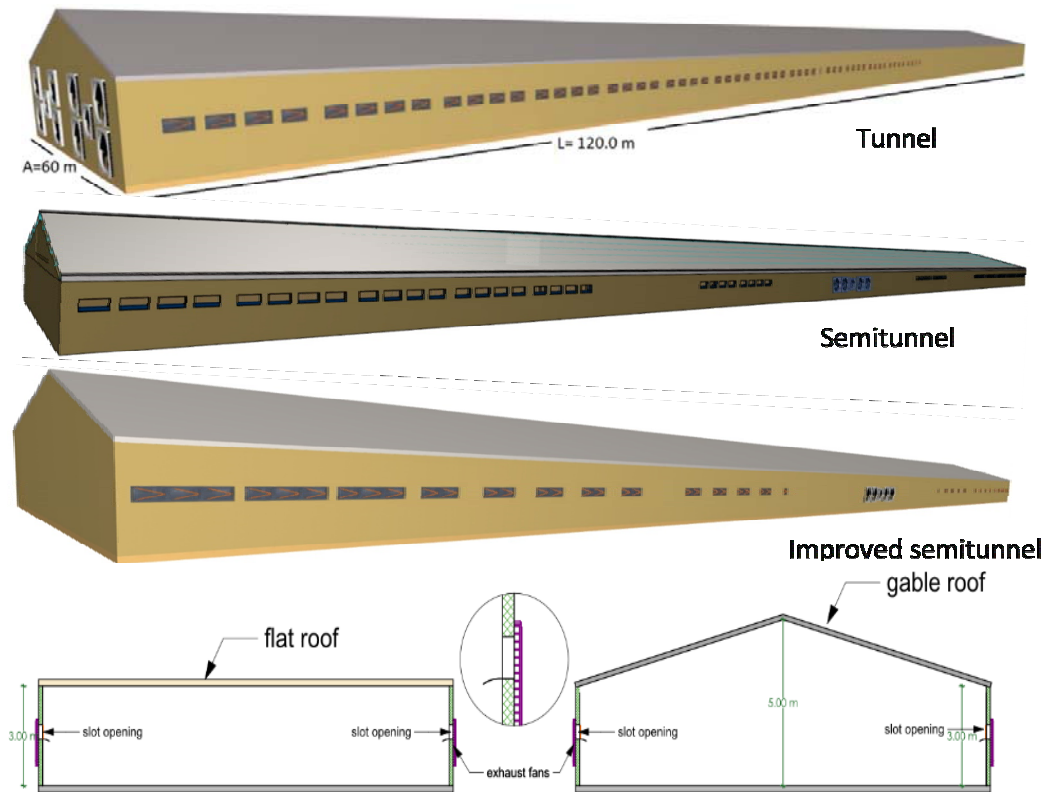


Figure 1. Tunnel (T), semi-tunnel (ST) and improved semi-tunnel (IST) configurations.

Table 1. Distribution of fans and windows in the three configurations.

Tunnel (T)	<ul style="list-style-type: none"> - Fourteen groups of slot openings on lateral sides in groups of four windows - Separation of 0.60m between groups - 50m wall free of windows- - 10 exhaust fans distributed vertically in the front axis.
Semi-tunnel (ST)	<ul style="list-style-type: none"> - Seven groups of slot openings on lateral sides in groups of four windows - Separation of 0.60m between windows - Separation of 10m between group windows the same characteristics - 5 Fans in the central axis defining a symmetry plane
Improved Semi-tunnel (IST)	<ul style="list-style-type: none"> - Long side had three groups of windows together. - Groups were of 3, 2 or 1 window according to distance to fans. - 5 exhaust fans uniformly distributed at the center of the building defining a symmetry plane

Table 2. Description of elements in the different analyzed geometries.

Elements	Design	Description
Roof	Flat (f)	Flat roof rectangle geometry at 3.0m height the ground.
	Gable (g)	The height of the side walls were 3.0m and roof top 5.0m
Windows Opening	Slot opening (S/O)	Rectangle windows of 0.4 x 0.9m, had height of the side walls 1.40m.
	With flap plate (F/P)	Flap plate in the rectangle slot opening of section, the flap had curvy of 40cm with 0° angle.

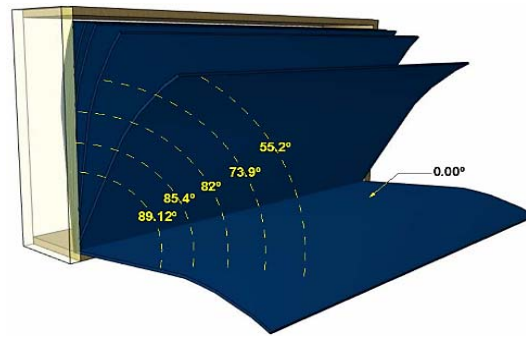


Figure 2. Different angles of slot opening with plate.

2.2 Computational fluid dynamic techniques

CFD simulations were used to analyze indoor environmental conditions according to the configurations of the ventilation system. These were computed for the T and ST configurations and then compared to the standard design (tunnel), both in winter and summer conditions. A half-section of the building was used as the three-dimensional computational domain with a symmetric wall.

Three-dimensional CFD grids were generated by StarCCM+ by CD-Adapco software (version 9.004.009). The CFD numerically solves the Reynolds-averaged form of the Navier–Stokes equations [16] within each cell in the domain, was used for the design of geometry, mesh structures tetrahedral of 0.4m, the mesh was refined in the flaps of the slot opening from 0.01-0.2m. The partial differential equations of the mass, momentum, and energy conservative equations were used to determine the fluid and energy transfers [17]. Eqs. (1)-(3) listed below are the mass, momentum and energy conservation equations solved in CFD simulations [16]. The measured data from theoretical information from the literature, were used for the initial and boundary conditions of the CFD model. The post-processor, was used for visualization of the air flow.

$$\frac{\partial \rho}{\partial t} + \nabla \cdot \rho \vec{v} = S_m \quad (1)$$

$$\frac{\partial(\rho \vec{v})}{\partial t} + \rho(\vec{v} \nabla) \vec{v} = -\nabla p + \nabla \cdot \bar{\tau} + \rho \vec{g} + \vec{F} \quad (2)$$

$$\bar{\tau} = \mu \left[(\nabla \vec{v} + \nabla \vec{v}^T) - \frac{2}{3} \nabla \cdot \vec{v} I \right] \quad (3)$$

where: ρ is the fluid density, kgm^{-3} ; \vec{v} is velocity; m.s^{-1} and S_m is mass source, kgm^{-3} ; t is time, s; τ the stress tensor, Pa; g gravitational; F is external force vector and I is the unit tensor, N m^{-3} and T is air temperature for the livestock building, $^{\circ}\text{C}$.

In the present study, the Realizable k - ϵ model was decided to be used as it satisfies certain mathematical constrains on the Reynolds stresses, and it is consistent with the physics of turbulent flows [18]. The input data for the CFD models are presented in Table 3, the sensible heat production of the broiler was determined using Eq (4) [19]. The effects of buoyancy in the model were activated.

$$\Phi_s = 0.61 \Phi_{\text{total}} - 0.228 * t^2 \quad (4)$$

where Φ_s is sensible heat production; Φ_{total} is total heat dissipation animal in animal houses, t is internal temperature.

The external air temperature (21.5°C in summer and 5°C in winter), air velocities at the exhaust fans and solid surfaces were used as the initial boundary conditions, as shown in Table 3. For each of the three geometries changes in the geometry were applied regarding the distribution of windows, fans, roof shapes and flaps angles of slot opening. The heat production was introduced in the model as a uniform flux of sensible heat from the concrete floor. Furthermore, the temperature and air velocity calculated at

broiler level were obtained for each CFD model and then statistically analyzed to determine the optimum options regarding temperature, air velocity, and comfort area using the index of temperature and velocity (ITV). As depicted in [20] ITV can be expressed as:

$$ITV = t_{db} \times V^{-0.058} \quad (5)$$

where: t_{db} is the dry bulb temperature °C and V is air velocity $m.s^{-1}$.

Comfortable limits were considered for ITV values within the range 18-25°C, and outside this interval the animals would be in discomfort therefore ITV higher than 30.1°C can accelerate heat stress for 24 hours and for ITV higher than 32.6°C and 35.5°C broilers have a critical thermal environment for 6 hours and 1 hour, respectively.

Table 3. Input data used for the CFD simulations.

Surface	Type	Properties
Windows	Outlet pressure	Summer: Outdoor temperature 21.5°C Winter: Outdoor temperature 5 °C
Fan center or 1.10m	Velocity	Velocity and direction (-3.92 m/s) Internal temperature 22°C
Fan side or 1.40m	inlet	Velocity and direction (- 6.87 m/s) Internal temperature 22°C
Ceiling polystyrene sandwich panel (¹ e = 5cm, ² λ = 0.033 W/m °K)		³ U = 0.58 W /m ² °K
Concrete walls consists: Precast concrete (e = 20cm; λ = 0.45 W /m °K), plaster cement (e = 4cm; λ = 0.4 W/m °K), insulating polyurethane (e = 2cm; λ = 0.04 W/m °K)	Wall	U = 0.81 W /m ² °K
Concrete floor (e = 2cm; λ = 2.5 W/m °K), insulating polystyrene (e=1.5 cm; λ = 0.046 W/m °K)		Heat flux sensible 101.94 W/m ²
Side wall symmetrical	Symmetry plane	

Where ¹e is thickness; ²λ is thermal conductivity W/m °K; ³U is thermal transmittance W/m² °K (adapted from Guerra [20]).

There, we combine Table 1 and Table 2, obtained 4 simulations for each poultry building (T, ST and IST) there were 12 in summer (21.5°C) and 12 in winter (5°C) (Table 4), a total number of 24 simulations were run.

Table 4. Simulations of tunnel (T), semi-tunnel (ST) and improved semi-tunnel (IST) configurations with different elements geometric.

Configuration	Roof type	Windows opening	
		Slot opening (S/O)	with flap plate (F/P)
Tunnel (T)	Flat (f)	S/O Tf _{s,w}	F/P Tf _{s,w}
	Gable (g)	S/O Tg _{s,w}	F/P Tg _{s,w}
Semi-tunnel (ST)	Flat (f)	S/O STf _{s,w}	F/P STf _{s,w}
	Gable (g)	S/O STg _{s,w}	F/P STg _{s,w}
Improved Semi-tunnel (IST)	Flat (f)	S/O ISTf _{s,w}	F/P ISTf _{s,w}
	Gable (g)	S/O ISTg _{s,w}	F/P ISTg _{s,w}

Where subindex h represent summer simulations and w represents winter simulations.

3. Results and discussion

3.1 Effect of roof shape

All parameters were estimated at a height of 0.2m (animal level). The roof shapes have an accelerating effect on air velocity as a consequence of the reduced section. However, this accelerating effect differs from one roof shape to another. When comparing flat and gable roof positions to each other, it can be noticed that the highest maximum increase in stream wise velocity occurred on flat roof in summer. However, in winter the highest air velocity occurred with gable roof with flaps plate in the slot opening (82° angle). According to Sosa [21] roof shape is important for natural ventilation and using gable roof takes advantage of better dynamics effect on wind ventilating interior environment. However, Norton [12] observed that during wind dominated ventilation the most over-ventilated regions in all buildings are situated closest to the gable walls. This is due to the incoming flow forming a boundary-layer flow at the gable wall as a result of the Coanda effect [22, 23]. The formation of a Coanda jet depends on aerodynamic and geometric parameters related to the inlet jet, the Reynolds number, and the distance of the inlet opening from the lateral wall [24, 25]. As a direct result of this phenomenon, the indoor airspeeds are increased closest to the gable wall [12]. Some studies focused on buildings with a gable roof and asymmetric opening positions can be consulted in the references; Peren [26] found that for wind-driven cross-ventilation, the airflow rate increases when increasing the roof inclination angle with more of 18° compared with flat roof. Also, Kindangen [27], observed that roof height has a strong influence on the indoor airflow in buildings with wind-driven natural ventilation. Under mechanical ventilation, however, the effect of the roof configuration has not been studied in depth and the main effects reported are based on reducing the section to increase air velocity, which is particularly interesting for summer conditions.

The results in summer (Table 5) indicate that tunnel configuration had on average higher air velocity at animal level using flat roof (S/O T_{fh}) (1.54 ± 0.74 m/s) than using gable roof (1.10 ± 0.49 m/s). These values were similar to Bustamante [11], who found at broiler level (0.25m height) higher average air velocity both using CFD (1.59 ± 0.68 m/s) and by means of direct measurements (1.55 ± 0.66 m/s). This system showed a uniform air exchange through the whole extent of the barn at high velocities in the same direction using negative pressure forced ventilation, but lower velocity in the semi-tunnel (ST) and improved semi-tunnel (IST) configurations.

Table 5. Average \pm standard deviation velocity (m/s), comfort area (%) at 0.20m of floor in summer of Tunnel (T), Semi tunnel (ST) and Improved Semi-tunnel (IST) configuration

Configuration	Roof type	Flap plate	Proportion of area attending to velocity [%]					Average [m/s]	
			<0.5 [m/s]	0.5-1.0 [m/s]	1.0-1.5 [m/s]	1.5-2.0 [m/s]	>2 [m/s]		
Tunnel (T)	Flat	No	13.27	15.94	12.85	21.15	36.78	49.95	1.54 \pm 0.74
		Yes	9.10	27.86	17.45	17.77	27.82	63.08	1.37 \pm 0.66
	Gable	No	13.24	31.02	24.95	30.23	0.57	86.19	1.10 \pm 0.49
		Yes	11.84	26.87	28.00	32.75	0.53	87.62	1.15 \pm 0.48
Semi-tunnel (ST)	Flat	No	18.30	47.47	33.83	0.40	0.00	80.05	0.83 \pm 0.32
		Yes	16.66	60.26	22.00	0.82	0.25	83.09	0.78 \pm 0.29
	Gable	No	27.40	60.64	11.14	0.73	0.10	72.50	0.77 \pm 0.30
		Yes	19.23	51.22	28.62	0.81	0.12	80.65	0.82 \pm 0.32
Improved Semi-tunnel (IST)	Flat	No	11.55	47.71	39.58	1.16	0.00	88.45	0.89 \pm 0.31
		Yes	16.56	64.59	18.13	0.58	0.14	83.30	0.77 \pm 0.26
	Gable	No	23.03	63.49	12.55	0.81	0.13	76.84	0.72 \pm 0.27
		Yes	17.95	54.53	26.55	0.79	0.19	81.86	0.79 \pm 0.31

The S/O T_{fh} configuration had a comfort area attending to air velocity (values ranging from 0.5-2.0 m/s) which was 49.9% with flat roof and raised until 86.2% when gable roof was considered. The area with air velocity over 2.0 m/s was highest (36.78%) when considering flat roof S/O. However, in general terms ST and IST configuration decreased the proportion of area at comfort velocity ranges (0.5-2.0m/s) when gable roof was installed, independently of the presence or absence of flaps. These two configurations had the highest proportion of area with air velocity within the range 0.5-1.0 m/s but the lowest with velocities higher than 1.5 m/s.

The T, ST, IST configurations with gable roof had the highest proportion of area in a comfort zone regarding to temperature (range from 18-25°C). However, when using with flat roof S/O we increased the proportion of area in the range 23-24°C. In contrast, using flat roof F/P and gable roof with or without flap plate increased the proportion of temperatures within the range 22-23°C. Tunnel configuration using flat roof F/P had higher area (12.0%) of temperature higher 25°C in comparison with ST and IST, whereas IST gable roof and flaps provided lower average temperature at animal level ($22.90 \pm 0.92^\circ\text{C}$) than when considering a flat roof (Table 6).

The tunnel using gable roof type had the highest comfort area at broiler height regarding the index of temperature and velocity (ITV ranging from 22 to 25°C) and this area was lowest with flat roof. Also, flat roof with flap plate increased area of ITV lower than 22°C (35.22%). Tunnel gable roof F/P had on average the lowest ITV ($22.94 \pm 1.30^\circ\text{C}$), but in contrast the IST configuration had higher comfort area considering ITV when compared with T and ST configurations (Table 7).

Table 6. Average \pm standard deviation temperature ($^\circ\text{C}$), comfort area (%) at 0.20m of floor in summer of Tunnel (T), Semi tunnel (ST) and Improved Semi-tunnel (IST) configuration.

Configuration	Roof type	Flap plate	Proportion of area attending to temperature [%]						Average [$^\circ\text{C}$]
			<22 [$^\circ\text{C}$]	22-23 [$^\circ\text{C}$]	23-24 [$^\circ\text{C}$]	24-25 [$^\circ\text{C}$]	>25 [$^\circ\text{C}$]	18-25 [$^\circ\text{C}$]	
Tunnel (T)	Flat	No	0.00	30.98	52.31	8.08	8.63	91.37	23.55 \pm 1.01
		Yes	5.46	61.80	12.92	7.85	11.97	88.03	23.18 \pm 1.31
	Gable	No	0.89	66.91	20.20	6.15	5.85	94.15	22.96 \pm 0.90
		Yes	3.68	63.91	18.87	5.88	7.66	92.82	22.96 \pm 1.0
Semi-tunnel (ST)	Flat	No	0.00	33.19	50.88	9.03	6.91	93.03	23.45 \pm 0.82
		Yes	5.48	49.43	22.79	11.42	10.89	89.11	23.24 \pm 1.22
	Gable	No	0.71	57.00	26.61	9.38	6.30	93.70	23.09 \pm 0.95
		Yes	1.97	60.92	23.33	7.21	6.57	93.43	23.14 \pm 1.0
Improved Semi-tunnel (IST)	Flat	No	0.00	33.56	53.79	7.17	5.48	94.52	23.37 \pm 0.79
		Yes	3.38	54.08	24.58	10.99	6.97	93.03	23.15 \pm 1.09
	Gable	No	3.98	61.03	22.47	8.11	4.41	95.59	22.93 \pm 0.9
		Yes	6.16	60.11	22.18	6.83	4.71	95.29	22.90 \pm 0.92

Table 7. Average \pm standard deviation ITV ($^\circ\text{C}$), comfort area (%) at 0.20m of floor in summer of Tunnel (T), Semi tunnel (ST) and Improved Semi-tunnel (IST) configuration

Configuration	Roof type	Flap plate	Proportion of area attending to ITV [%]					Average [$^\circ\text{C}$]
			<22 [$^\circ\text{C}$]	22-25 [$^\circ\text{C}$]	25-30 [$^\circ\text{C}$]	>30 [$^\circ\text{C}$]	18-25 [$^\circ\text{C}$]	
Tunnel (T)	Flat	No	27.05	56.79	16.11	0.05	83.83	23.24 \pm 1.54
		Yes	35.22	52.75	12.02	0.01	87.97	22.96 \pm 1.52
	Gable	No	9.25	82.06	8.67	0.02	91.32	23.01 \pm 1.20
		Yes	14.76	75.73	9.50	0.02	90.48	22.94 \pm 1.30
Semi-tunnel (ST)	Flat	No	0.00	85.75	14.06	0.19	84.23	23.85 \pm 1.17
		Yes	3.32	77.89	18.75	0.04	81.27	23.71 \pm 1.51
	Gable	No	0.53	83.85	15.57	0.05	84.38	23.6 \pm 1.49
		Yes	11.56	74.63	13.65	0.17	86.18	23.44 \pm 1.48
Improved Semi-tunnel (IST)	Flat	No	0.00	90.36	9.59	0.05	90.36	23.64 \pm 0.98
		Yes	1.48	83.48	14.60	0.44	84.96	23.61 \pm 1.39
	Gable	No	2.09	85.59	12.23	0.08	87.69	23.51 \pm 0.9
		Yes	11.78	76.33	11.79	0.09	88.11	23.35 \pm 1.35

In the winter period outside temperatures was set to 5°C in the three configurations. The use of gable roof increased slightly air velocity at animal level (Table 8) and compared to flat roof it showed on average higher air velocity (S/O T_{g_w} , 0.31 ± 0.07 m/s). Air velocity was lowest for S/O IST_{f_w} (0.24 ± 0.05 m/s). ST and IST configuration increased comfort area in terms of temperature using flat roof, but this was lowest

with gable roof (velocities of 0.1-0.3 m/s), IST presented the lowest area of velocities within the range 0.3-0.5 m/s.

The S/O tunnel gable roof model showed the lowest average temperature ($17.83\pm 3.25^{\circ}\text{C}$), whereas ST gable roof S/O had the highest ($19.35\pm 2.67^{\circ}\text{C}$) (Table 9). We also observed that the area with temperature lower than 18°C and in the range $18-25^{\circ}\text{C}$ was lowest in tunnel configuration (T), and higher in ST and IST. In cold season Seo [10] observed in a conventional model a temperature of 21.5°C at 0.20 m height. Also, Mostafa [12] found for a standard design an average temperature in the broiler zone of 23.9°C . As expected, the lowest temperature was located close to the inlet slots and the highest temperature was located close to the exhaust fans by dragging sensible heat loss.

In our analysis, the tunnel gable roof S/O configuration showed on average lower proportion of area with ITV in the comfort interval ($18-25^{\circ}\text{C}$) and ITV was on average $19.14\pm 3.57^{\circ}\text{C}$. We also observed that tunnel with gable roof had more area with ITV lower than 18°C and ITV in the range $25-30$. The S/O ST gable roof configuration had highest average ITV ($20.81\pm 2.86^{\circ}\text{C}$) and area of ITV in the comfort interval (93.04%), as show Table 10.

Table 8. Average \pm standard deviation velocity (m/s), comfort area (%) at 0.20m of floor in cold of Tunnel (T), Semi tunnel (ST) and Improved Semi-tunnel (IST) configuration.

Configuration	Roof type	Flap plate	Proportion of area attending to velocity [%]				Average [m/s]
			<0.1 [m/s]	0.1-0.3 [m/s]	0.3-0.5 [m/s]	>0.5 [m/s]	
Tunnel (T)	Flat	No	0.61	59.19	40.20	0.00	0.27 ± 0.09
		Yes	1.09	69.90	29.01	0.00	0.25 ± 0.09
	Gable	No	0.86	39.36	59.77	0.01	0.31 ± 0.07
		Yes	1.46	53.14	45.40	0.00	0.28 ± 0.08
Semi-tunnel (ST)	Flat	No	1.54	70.05	28.40	0.00	0.26 ± 0.07
		Yes	1.65	70.68	27.66	0.00	0.26 ± 0.08
	Gable	No	0.36	50.98	48.58	0.08	0.29 ± 0.06
		Yes	0.72	52.96	46.30	0.02	0.28 ± 0.06
Improved Semi-tunnel (IST)	Flat	No	0.99	86.85	12.15	0.01	0.24 ± 0.05
		Yes	2.45	81.25	16.30	0.00	0.24 ± 0.06
	Gable	No	0.21	72.23	27.27	0.28	0.27 ± 0.05
		Yes	1.04	77.85	21.11	0.00	0.26 ± 0.06

Table 9. Average \pm standard deviation temperature ($^{\circ}\text{C}$), comfort area (%) at 0.20m of floor in cold of Tunnel (T), Semi tunnel (ST) and Improved Semi-tunnel (IST) configuration.

Configuration	Roof type	Flap plate	Proportion of area attending to temperature [%]					Average [$^{\circ}\text{C}$]	
			<18 [$^{\circ}\text{C}$]	18-20 [$^{\circ}\text{C}$]	20-22 [$^{\circ}\text{C}$]	22-25 [$^{\circ}\text{C}$]	>25 [$^{\circ}\text{C}$]		
Tunnel (T)	Flat	No	56.47	16.60	10.82	15.03	1.08	42.45	18.05 ± 3.25
		Yes	56.94	16.51	10.56	15.00	0.99	42.07	18.27 ± 2.97
	Gable	No	60.15	13.59	10.76	14.83	0.68	39.18	17.83 ± 3.25
		Yes	61.09	13.20	10.43	14.63	0.65	61.74	17.99 ± 3.03
Semi-tunnel (ST)	Flat	No	42.10	23.57	17.91	14.91	1.52	56.39	18.85 ± 2.91
		Yes	43.05	23.57	17.37	14.39	1.62	55.33	18.84 ± 2.86
	Gable	No	32.76	26.22	21.94	18.46	0.61	66.63	19.35 ± 2.67
		Yes	36.22	24.42	20.46	18.11	0.78	63.0	19.25 ± 2.68
Improved Semi-tunnel (IST)	Flat	No	46.58	18.89	14.11	17.27	3.16	50.26	18.57 ± 3.58
		Yes	47.35	22.07	13.85	14.97	1.77	50.88	18.45 ± 3.24
	Gable	No	35.98	25.43	19.67	18.15	0.77	63.25	19.16 ± 2.81
		Yes	37.00	26.08	18.91	17.34	0.67	62.33	19.10 ± 2.74

Table 10. Average \pm standard deviation ITV ($^{\circ}$ C), comfort area (%) at 0.20m of floor in cold of Tunnel Tunnel (T), Semi tunnel (ST) and Improved Semi-tunnel (IST) configuration.

Configuration	Roof type	Flap plate	Proportion of area attending to ITV [%]					Average [$^{\circ}$ C]	
			<18	18-22	22-25	25-30	>30		
			[$^{\circ}$ C]	[$^{\circ}$ C]	[$^{\circ}$ C]	[$^{\circ}$ C]	[$^{\circ}$ C]		
Tunnel (T)	Flat	No	41.84	31.31	14.61	12.14	0.10	87.77	19.55 \pm 3.80
		Yes	39.42	33.99	14.49	12.00	0.09	87.91	19.88 \pm 3.42
	Gable	No	45.52	31.31	14.27	8.84	0.05	91.11	19.14 \pm 3.57
		Yes	45.64	31.00	13.70	9.58	0.07	90.35	19.40 \pm 3.32
Semi-tunnel (ST)	Flat	No	26.44	41.06	22.60	9.68	0.22	90.10	20.43 \pm 3.31
		Yes	25.78	43.03	20.48	10.41	0.30	89.30	20.44 \pm 3.25
	Gable	No	19.50	45.68	27.85	6.96	0.00	93.04	20.81 \pm 2.86
		Yes	20.93	44.83	26.69	7.54	0.00	92.46	20.76 \pm 2.86
Improved Semi-tunnel (IST)	Flat	No	31.86	34.25	21.04	12.36	0.49	87.15	20.21 \pm 3.97
		Yes	31.04	38.95	19.79	9.93	0.29	89.78	20.10 \pm 3.55
	Gable	No	20.79	45.05	26.12	8.04	0.00	91.96	20.68 \pm 3.03
		Yes	20.05	47.10	25.32	7.53	0.00	92.47	20.66 \pm 2.88

3.2 Analysis with inlet flaps

The main function of ventilation is to allow the exchange of air with the outside, which contributes to control indoor temperature, moisture and the concentration of pollutant gases. Air inlets are essential in defining the direction of the incoming airflow, and in maintaining the thermal condition into the animal occupied zone by providing sufficient inlet air velocity. Changing the size of the slot opening or the type of inlet affected the direction and magnitude of inlet air velocity both in winter and summer simulations [8]. The flap plates affected the direction of the incoming air as shown Figure 3. When windows have no flaps the velocity is accelerated and directed downward immediately after passing through the opening. As predicted by Karava and Stathopoulos [28], the air flow trajectory lowered when windows are close to fans as a consequence of the higher depression. These variations depended the geometry of the openings, while the pressure coefficients depend on the overall geometry of the building, the location of the windows in the building itself, and the wind incidence on the building [29].

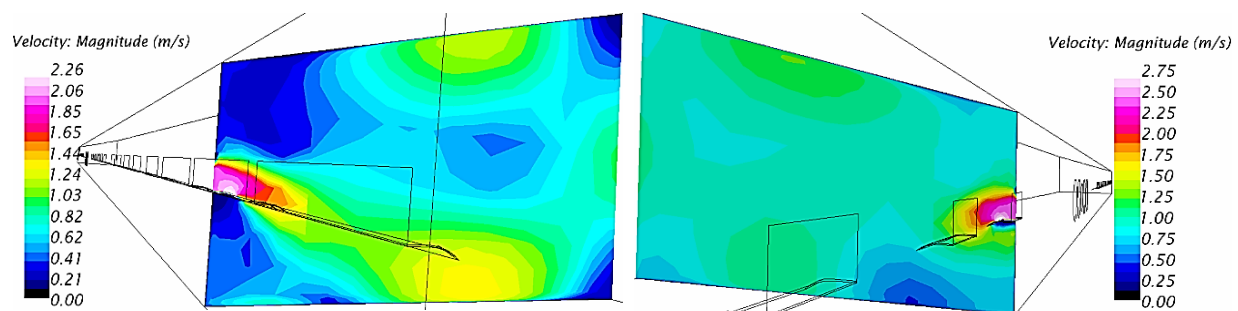


Figure 3. Air velocity distribution in the IST configuration using flap plate, at two vertical planes located at the furthest window (left) and closest window (right) to the fans.

During the summer period, the IST S/O configuration using flat roof showed the highest proportion of area at comfort regarding air velocity (0.5 – 2 m/s). In this case, no flap plates were considered and air entered directly without obstacle. This effect was less evident when using gable roof. The effect of considering flap plates in T, ST and IST configuration was a decrease of the proportion of the area at temperatures between 23 and 24 $^{\circ}$ C. ISTg_s configuration showed the highest proportion of area at comfort regarding temperature (18-25 $^{\circ}$ C). Similarly, the addition of flaps increased the area of ITV<22 $^{\circ}$ C in all configurations.

In the winter period, the flap plate in the inlet windows increased the air velocity of the incoming air. According to Rufes [30] when the inlet is located higher in the wall, the flap plate with different deflection angle directed the incoming air stream across the ceiling, regardless of the outlet. This will govern the direction of the indoor air stream and this will be independent of the outlet opening position.

In Figure 4 it is shown that the use of flap plates in winter conditions regulate air flow rate in vertical projection on walls and roof producing a phenomenon adhesion of air on the surface due to the existence lower pressures in the space comprised between surface and air flow [31]. Therefore, the increasing velocity gradient at the walls was completely attributable to the augmentation of the airflow rate [32].

In all configurations (T, ST and IST) the flap increased the area of air velocity within the range 0.1-0.3 m/s and decreased area with velocities of 0.3-0.5 m/s. However, the effect of flap plates in the IST flat roof model decreased the proportion of area with velocities from 0.1 to 0.3 m/s and increased it when using gable roof. We also observed that the flap plate at the inlet windows increased the area of temperature <18°C and decreased with temperature 18-25°C for T and ST configurations. In contrast, IST configuration increased the area of temperatures between 18 and 20°C, and decreased the area between 20 and 25°C.

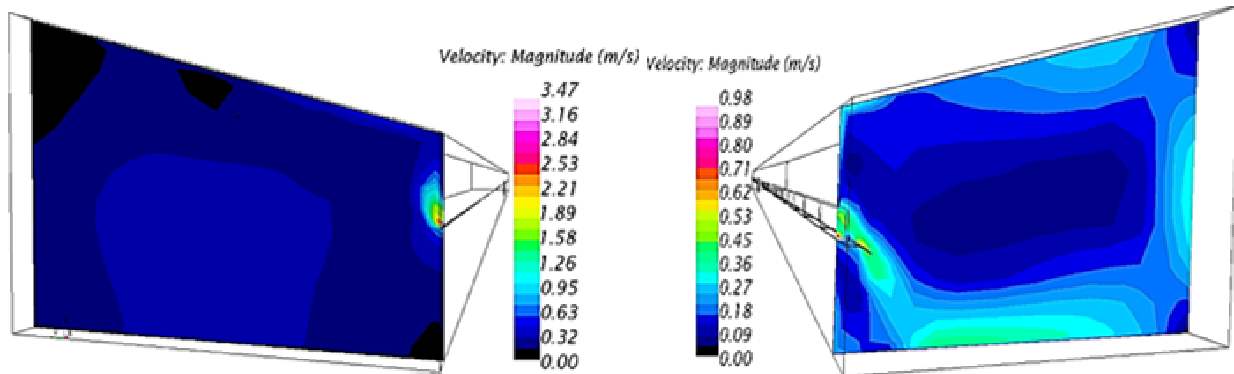


Figure 4. Effect of flap angle (89°, left and 0°, right) on air velocity.

3.2.1 Effect slot opening angle

The IST configuration registered a slight variation in the average in air velocity at animal level (0.26 m/s) when considering different angles from 0° to 89° at 0.20m of floor (Table 11). The velocity was highest at the inlet and decreased gradually when the stream entered the building next to the roof. The center of the stream continued moving at a similar velocity to the entrance, while the outer edges of the stream are slowed down by friction and turbulent mixing with the surrounding air. The flap plate angle of 73.9° registered the highest area of velocities between 0.1-0.3 m/s at animal level, whereas the angle 40° increased the area with air velocities between velocities 0.3-0.5 m/s. There were small differences in pressure distribution. The warm air has less density and ascended, which facilitated the cold air inlet by to drop due to the higher density and mix with the rest of the air [33]. Therefore, air close to the ceiling mixes with the fresh incoming air before it reaches to the broiler zone. However, the differential pressures did not seem to affect air velocity at 0.2m above floor level of the broiler house [34].

Table 11. Average \pm standard deviation of air velocity (m/s), and distribution of area regarding different velocity intervals (%) at 0.20m of floor in winter for IST configuration for different window opening angles.

Flap plate angle	Comfort area velocity [%]				Average [m/s]
	<0.1 [m/s]	0.1-0.3 [m/s]	0.3-0.5 [m/s]	>0.5 [m/s]	
89°	1.10	72.79	26.11	0.00	0.261 \pm 0.07
85.4°	1.10	76.17	22.73	0.00	0.262 \pm 0.06
82°	1.04	77.85	21.11	0.00	0.260 \pm 0.06
73.9°	0.63	81.06	18.31	0.00	0.259 \pm 0.05
55.2°	0.18	74.78	25.05	0.00	0.260 \pm 0.05
0°	1.19	69.26	28.76	0.79	0.270 \pm 0.08

Logically, the largest air velocity happened when small inlets and large outlets were simultaneously considered. The total force is acting on a small area and forcing air through the opening at a high pressure. This effect was lower when flaps were open (Figure 4). If the inlet opening is large, air velocity

will be lower as a consequence of the higher section, but the airflow rate increases in any case. Also, Kwon [8] observed that changing the opening angle affected the distance travelled by the incoming cold air before mixing with the rest of the air. This indicated that the initial angle of the window flaps could influence the mixing behavior of cold and warm air, and therefore affecting the resulting inside air temperature at animal level.

Regarding the conditions potentially experimented by the animals, reducing the opening (89°) involved the highest average temperature at animal level (on average $20.28 \pm 2.5^\circ\text{C}$, see Table 12). This also involved a more homogeneous distribution of temperature and ITV (Table 13). On the contrary, opening the window flaps (0°) increased the area with temperature lower than 18°C , which is related to increased losses of sensible heat in winter conditions. The average temperatures obtained in this study are similar to those reported by Song [35], who found $19.7 \pm 1.21^\circ\text{C}$ in a tunnel configuration using flaps and described similar behavior of inlet air flow depending on window characteristics.

Table 12. Average \pm standard deviation of temperature ($^\circ\text{C}$), and distribution of area regarding different velocity intervals (%) at 0.20m of floor in winter for IST configuration for different window opening angles.

Flap plate angle	Comfort area temperatura [%]						Average [$^\circ\text{C}$]
	<18 [$^\circ\text{C}$]	18-20 [$^\circ\text{C}$]	20-22 [$^\circ\text{C}$]	22-25 [$^\circ\text{C}$]	>25 [$^\circ\text{C}$]	18-25 [$^\circ\text{C}$]	
89°	25.76	25.32	24.44	23.06	1.41	72.82	20.28 ± 2.5
85.4°	38.44	23.84	18.80	18.24	0.67	60.89	19.0 ± 2.93
82°	37.00	26.08	18.91	17.34	0.67	62.33	19.1 ± 2.74
73.9°	36.14	25.54	19.15	18.50	0.67	63.19	19.16 ± 2.82
55.2°	34.92	25.24	20.23	18.74	0.87	64.21	19.26 ± 2.81
0°	40.46	30.49	20.41	8.62	0.03	59.66	18.7 ± 2.26

Table 13. Average \pm standard deviation of ITV ($^\circ\text{C}$), and distribution of area regarding different velocity intervals (%) at 0.20m of floor in winter for IST configuration for different window opening angles.

Flap plate angle	Comfort area ITV [%]						Average [$^\circ\text{C}$]
	<18 [$^\circ\text{C}$]	18-22 [$^\circ\text{C}$]	22-25 [$^\circ\text{C}$]	25-30 [$^\circ\text{C}$]	>30 [$^\circ\text{C}$]	18-25 [$^\circ\text{C}$]	
89°	10.18	42.64	34.98	12.20	0.00	87.80	21.74 ± 2.74
85.4°	22.56	43.51	25.42	8.51	0.00	91.49	20.56 ± 3.11
82°	20.05	47.10	25.32	7.53	0.00	92.47	20.66 ± 2.88
73.9°	19.57	45.72	26.14	8.57	0.00	91.43	20.74 ± 3.01
55.2°	18.84	44.65	28.16	8.34	0.00	91.66	20.84 ± 2.99
0°	20.03	54.70	22.80	2.46	0.00	97.63	20.22 ± 2.42

4. Conclusions

The CFD results demonstrate the performance of different distribution of elements for summer and winter conditions. The relative position of windows and fans, the roof shape, and inlet window properties were studied. All these parameters affected the distribution and homogeneity of ambient parameters (temperature, air velocity and ITV). In general terms, the IST configuration provided better results for summer conditions due to a better distribution of air velocity. Roof type (flat or gable roof) also affected wind distribution and using flat roof tended to increase wind velocity. Finally, reducing window opening increased the homogeneity of ambient parameters at animal level, which is considered to be of particular interest under winter conditions. Increasing window opening also increased the average air velocity at animal level and decreased the ambient temperature, which is undesirable under winter conditions. Further validation of the different models and comparisons with CFD is the next step. Nevertheless, this tool can be used to simulate and optimize different ventilation systems.

References

- [1] Abreu P.G. De, Maria V, Abreu N, et al. Revista Brasileira de Zootecnia Curtain color and lighting program in broiler production □: III - thermal comfort. 2011:2026-2034.

- [2] Yahav S., Straschnow A., Vax E., Razpakovski V. and D. Shinder. Air velocity alters broiler performance under harsh environmental conditions. *Poultry science*. 2001, 80 (6): 724-726.
- [3] William J., Olsen W. Improving commercial broiler attic inlet ventilation through data acquisition coupled. 2012.
- [4] Mazanowski A. Modern broiler chicken production. Ed. Pro Agricola, Gerzwald. 2011: 246.
- [5] Osorio H. R., Ferreira T. I. de F., Osorio S. J. A., Oliveira R. K. S., Guerra G. L. M. Modeling of the Thermal Environments in Shed Negative Pressure Tunnel Type of Chicks. *Revista Facultad Nacional de Agronomía Medellín*. 2013, 66 (2):7085-7093.
- [6] Bjerg B, Svidt K, Zhang G, Morsing S, Johnsen JO. Modeling of air inlets in CFD prediction of airflow in ventilated animal houses. *Comput Electron Agric*. 2002, 34(1-3):223-235.
- [7] Wisate C, Suntivarakorn R, Winitchai S. Improvement of Air Change Rate Efficiency for a Broiler House with Multi Inlet System. *Adv Sci Lett*. 2013, 19(9):2699-2702.
- [8] Kwon K, Lee I, Zhang GQ, Ha T. Computational fluid dynamics analysis of the thermal distribution of animal occupied zones using the jet-drop-distance concept in a mechanically ventilated broiler house. *Biosyst Eng*. 2015, 136:51-68.
- [9] Mostafa E, Lee I-B, Song S-H, et al. Computational fluid dynamics simulation of air temperature distribution inside broiler building fitted with duct ventilation system. *Biosyst Eng*. 2012, 112(4):293-303.
- [10] Seo I. H., Lee I. B., Moon O. K., Kim H.T., Hwang H. S., Hong S. W., Bitog J., Yoo J. I., Kwon K. S., Kim Y. H., Han J. W. Improvement of the ventilation system of a naturally ventilated broiler house in the cold season using computational simulations. *Biosystems Engineering*. 2009, 104 (1):106-117.
- [11] Bustamante E, García-Diego F-J, Calvet S, Torres A, Hospitaler A. Measurement and Numerical Simulation of Air Velocity in a Tunnel-Ventilated Broiler House. *Sustainability*. 2015, 7(2):2066-2085.
- [12] Norton T, Grant J, Fallon R, Sun DW. Assessing the ventilation performance of a naturally ventilated livestock building with different eave opening conditions. *Comput Electron Agric*. 2009:1-15.
- [13] Álvarez M. A. J. Estudio de las características geométricas y del comportamiento aerodinámico de las mallas antiinsectos utilizadas en los invernaderos como media de protección vegetal. Tesis doctoral. Universidad de Almería, 2009.
- [14] Oliveira Rocha, K. S., Ferreira Tinôco, I. de F., Helvecio Martins, J., Osorio Saraz, J. A., Arêdes Martins, M. Modeling and simulation of internal environment conditions in high-density poultry houses with ventilation using computational fluid dynamics. *International Conference of Agricultural Engineering*. Zurich 6-10 July, 2014.
- [15] Bjerg B, Liberati P, Marucci A, et al. Modelling of ammonia emissions from naturally ventilated livestock buildings: Part 2, air change modelling. *Biosyst Eng*. 2013, 116(3):246-258.
- [16] Launder B. E., Spalding D. B. The numerical computation of turbulent flows. *Computer Methods in Applied Mechanics and Engineering*. 1974, 3:269-289.
- [17] Lee, I. B., and T. Short. 2000. Two-dimensional numerical simulation of natural ventilation in a multi-span greenhouse. *Trans. ASAE* 43(3): 745-753.
- [18] Lee I, Sase S, Sung S. Evaluation of CFD Accuracy for the Ventilation Study of a Naturally Ventilated Broiler House. 2007, 41(October 2005):53-64.
- [19] Pedersen S., Sällvik K. 4th Report of Working Group on Climatization of Animal Houses. *International Commission of Agricultural Engineering, Section II*. 2002.
- [20] Guerra-Galdo E. H., Calvet S. S., Estellés B. F., López-Jiménez P. A. CFD model for ventilation assessment in poultry houses with different distribution of windows. *International Journal Energy and Environment*. 2015, 6 (5): 411-424.
- [21] Sosa G. M. E. Ventilación natural efectiva y cuantificable. *Comfort térmico en climas cálidos-húmedos*. Universidad Central de Venezuela. Gráficas León SRL. 1999.
- [22] Newman B. G. The deflection of plane jets by adjacent boundaries-Coanda effect. In *Boundary Layer and Flow Control* (ed. G. V. Lachmann), vol 1 pp 232-264. Pergamon.
- [23] Wille R., Fernholz H. (1965) Report on the first European Mechanics Colloquium, on the Coanda effect. *J. Fluid Mech*. 1961, 23:801-819.
- [24] Awbi Hazim. *Ventilation and Building*. Spon Press. London and New York. 1991.

- [25] Moureh J., Flick D. Airflow characteristics within a slot-ventilated enclosure, *Int. J. Heat Fluid Flow*. 2005, 26:12-24.
- [26] Peren J. I., Van Hooff T., Leite B. C. C., Blocken B. CFD analysis of cross-ventilation of a generic isolated building with asymmetric opening positions: impact of roof angle and opening location. *Building and Environment*. 2014: 1-21.
- [27] Kindangen J., Krauss G., Depecker P. Effects of roof shapes on wind-induced air motion inside buildings. *Build Environ*. 1997, 32: 1-11.
- [28] Karava P. and Stathopoulos T. Wind-Induced Internal Pressures in Buildings with Large Façade Openings. *Journal of Engineering Mechanics*. 2012, 138 (4).
- [29] Demmers T., Phillips V., Short L., Burgess L., Hoxey R., Wathes C. Validation of ventilation rate measurement methods and the ammonia emission from naturally ventilated dairy and beef buildings in the United Kingdom. *Journal of Agricultural Engineering Research*. 2001, 79(1): 107-116.
- [30] Rufes M. P. *Difusión del aire en locales*. Ediciones CEAC. Barcelona.1999.
- [31] Escorihuela J., Esteban J. L., Futos J. M., Olaya M., Torroja B. *Bases para el Diseño Solar pasivo*. GRAFIMAD Madrid. 1983.
- [32] Van Overbeke P., Pieters J. G., De Vogeleer G., Demeyer P. Development of a reference method for airflow rate measurements through rectangular vents towards application in naturally ventilated animal houses: Part 1: Manual 2D approach. *Computers and Electronics in Agriculture* Volume. 2014, 106:31-41.
- [33] Bruce, J. M. Ventilation of a model livestock building by thermal buoyancy. *Trans. ASAE*.1982, 25(6):1724-1726.
- [34] Blanes-Vidal V. Differential pressure as a control parameter for ventilation in poultry houses: effect on air velocity in the zone occupied by animals. *Spanish Journal of Agricultural Research*. 2007, 5(1):31-37.
- [35] Song S.-H. , Lee I.-B., Hwang H.-S., Hong S.-W., Seo I.-H., Bitog J.P. , Kwon K.-S., Choi J.-S. CFD analysis and comparison of forced-ventilation systems of poultry houses in Korea XVIIth World Congress of the International Commission of Agricultural and Biosystems Engineering (CIGR). 2010.



Eva Hilda Guerra-Galdo received Master's Degree in Animal Production in the Department of Animal Science and Technology from Universitat Politècnica de València. She is pursuing Doctoral Degree in Animal Science and Technology from Universitat Politècnica de València. She is researching about the modeling of air flow and temperature in poultry buildings. This project is cofounded by PRONABEC of Perú.
E-mail address: ehgg.-@hotmail.com



Fernando Estéllés Barber is Agricultural Engineer (2007), MSc on Livestock Production (2007) and PhD (2010) at Universitat Politècnica de València (Spain) His areas of research are Livestock and Environment, and Climate control in livestock farms. He leads a project on optimizing dairy cows' farm buildings to cope with climate change consequences (Optibarn). He also participates on other projects related to gaseous emission from manure and collaborates with the development of Spanish Emissions Inventories. He has published about 25 scientific articles in indexed (JCR) journals as well as several dissemination articles on his topics of research. He has also participated in many international conferences in his area. Dr. Estellés is one of the Spanish representatives of the Inventories and Monitoring workgroup on the Global Research Alliance on Agricultural Greenhouse Gases. He is also member of the board of the scientific society "Remedia" (Spanish Network for Mitigation of Climate Change in Agroforestry).
E-mail address: feresbar@upvnet.upv.es



Salvador Calvet Sanz is Agricultural Engineer (2003) and PhD in Animal Science (2008) at Universitat Politècnica de València (Spain). His areas of research are Livestock and Environment, and Climate control in livestock farms. He leads a project on evaluating how animal feeding is related to environmental impacts of livestock production. In the past he has leaded and participated in other projects related to emissions to the atmosphere, emission inventories or climate control. He has published 28 scientific articles in indexed (JCR) journals as well as several dissemination articles on his topics of research. He has also participated in many international conferences in his area. Dr. Calvet is secretary of the CIGR (International Commission of Agricultural Engineering) Working Group on Hot Climates and participates in scientific societies “Remedia” (Spanish Network for Mitigation of Climate Change in Agroforestry), CIGR and EurAgEng (European Society of Agricultural Engineers).

E-mail address: salcalsa@upvnet.upv.es



Petra Amparo López-Jiménez is M.Sc. and PhD in Industrial Engineering, Associate Professor in the Hydraulic and Environmental Engineering Department at the Universitat Politècnica de València. She is currently the Associate Director of the Hydraulic and Environmental Engineering Department of Universitat Politècnica de València. She has more than a decade of experience in research and teaching in Engineering fields, always related to hydraulic topics. She is author and editor of several publications about Hydraulic an Environmental Engineering and Flow Dynamics. She has participated in national and international R&D projects and co-organized International Seminars and Networks. She is an experienced University Teacher, an active researcher and a former practicing engineer.

E-mail address: palopez@upv.es